

Supporting Information
©Wiley-VCH 2016
69451 Weinheim, Germany

Understanding the Role of Internal Diffusion Barriers in Pt/Beta Catalyzed Isomerization of *n*-Heptane

Zhongyuan Guo, Xin Li, Shen Hu, Guanghua Ye*, Xinggui Zhou, and Marc-Olivier Coppens*

Abstract: Applications of zeolites in catalysis are plagued by strong diffusion resistance, which results from limitations to molecular transport in micropores, across external crystal surfaces, but also across internal interfaces. The first type of diffusion resistance is well understood, the second is receiving increasing attention, while the diffusion barriers at internal interfaces remain largely unclear. We take Pt/Beta catalyzed isomerization of *n*-heptane as the model system to explore the role of internal diffusion barriers in zeolite catalysis. The two as-synthesized Pt/Beta catalysts have an identical Pt loading, similar Beta particle size and acidity, but different internal structures. A Pt/Beta crystal with no observable internal interfaces can be 180% higher in activity and 22% higher in selectivity than its counterpart with numerous internal interfaces. This can only be attributed to the strong transport barriers across internal interfaces, as supported by directly comparing the apparent diffusivities of the two Beta samples.

DOI: 10.1002/anie.2016XXXXX

Table of Contents

1. Experimental Procedures.....	S3
1.1. Catalyst synthesis.....	S3
1.2. Catalyst characterization.....	S4
1.3. Catalytic tests.....	S6
1.4. ZLC measurements.....	S6
2. Results and Discussion.....	S8
2.1. Characteristics of Beta samples.....	S8
2.2. Pt particle size.....	S9
2.3. Elimination of the effect of Pt.....	S11
2.4. Catalytic performance.....	S13
2.5. ZLC results.....	S14
3. References.....	S15
4. Author Contributions.....	S16

SUPPORTING INFORMATION

1. Experimental Procedures

1.1. Catalyst synthesis

Beta zeolites

Polycrystalline and single-crystalline Beta zeolites were synthesized using the hydrothermal method. An appropriate amount of silica (34 wt% in aqueous solution, Sigma-Aldrich) was added into the solution containing deionized water, tetraethylammonium hydroxide (TEAOH) (25 wt% in aqueous solution, Shanghai Cainorise Chemicals Co., Ltd.), and sodium hydroxide (≥ 96.0 wt%, Sinopharm Chemical Reagent Co., Ltd.). Then, the dissolved sodium aluminate ($\text{Al}_2\text{O}_3 \geq 41$ wt%, Sinopharm Chemical Reagent Co., Ltd.) was dropwise added into the solution, and the solution was stirred for 3 h at room temperature. For both Beta zeolites, the molecular composition of the final mixture was $1\text{SiO}_2:0.36\text{TEAOH}:0.106\text{NaOH}:0.02\text{Al}_2\text{O}_3:11.8\text{H}_2\text{O}$, and this final mixture was hydrothermally treated in a Teflon-lined, stainless steel autoclave under different hydrothermal conditions (see Table S1). After the hydrothermal treatment, the product was washed with deionized water and centrifuged, which was repeated three times, and then the product was dried at 353 K for 8 h. Finally, to remove the organic template, the product was calcined in air at 823 K for 6 h with a temperature ramp of 1.5 K/min.

The protonated Beta zeolites were obtained through ion exchange of the calcined product with a solution of 1 M NH_4Cl at 353 K for 8 h, followed by centrifugation, drying at 353 K for 8 h, and calcination at 823 K for 4 h (temperature ramp 1.5 K/min). The as-synthesized polycrystalline and single-crystalline Beta samples were labeled as Beta-A and Beta-B, respectively.

Table S1. Molecular composition of reaction mixture and hydrothermal conditions for preparing Beta zeolite samples.

BEA-type zeolite	Reagent		Molecular composition of reaction mixture	Temperature (K)	Time (days)
	Si	Al	SiO_2 : TEAOH: NaOH: Al_2O_3 : H_2O		
Beta-A	Silica sol	NaAlO_2	1:0.36:0.106:0.02:11.8	413	3
Beta-B	Silica sol	NaAlO_2	1:0.36:0.106:0.02:11.8	393	8

SUPPORTING INFORMATION

Platinum loading

The as-synthesized Beta samples were loaded with 0.5 wt% Pt by incipient wetness impregnation with a solution of H₂PtCl₆ (Sigma-Aldrich). Afterwards, the samples were aged for 12 h, dried at 353 K for 8 h, and calcined in air at 723 K for 3 h. Finally, the samples were reduced in H₂ flow at 723 K for 2.5 h. The two samples were labeled as Pt/Beta-A and Pt/Beta-B. The Pt loading of the two catalysts is sufficient to make the dehydrogenation and hydrogenation reactions reach equilibrium, and isomerization over acid sites is the rate determining step.^[1-4] Pt dispersions and particle sizes of the catalysts are summarized in Table S2.

1.2. Catalyst characterization*XRD*

X-ray diffraction (XRD) patterns were recorded using a D8 advance A25 diffractometer (Bruker, Germany) equipped with a Cu K α radiation source, and the measurements were conducted in the range $3^\circ < 2\theta < 50^\circ$ at a rate of 1.2°/min.

SEM

Scanning electron microscopy (SEM) images were taken using a NOVA Nano SEM450 microscope (FEI, USA) operating at 3 kV.

HRTEM

High-resolution transmission electron microscopy (HRTEM) images were taken using a JEM 2100 instrument (JEOL, Japan) operating at 200 kV.

HAADF-STEM

High-angle annular dark-field scanning transmission electron microscopy (HAADF-STEM) was performed on a Tecnai G2 F20 S-Twin equipped with a digitally processed STEM imaging system.

N₂ adsorption and desorption

SUPPORTING INFORMATION

N₂ adsorption and desorption measurements were performed at a temperature of 77 K using an ASAP 2020 instrument (Micromeritics, USA). Prior to the measurements, the samples were degassed at 1.33×10^{-3} Pa and 523 K for 6 h. The total pore volumes were determined from the N₂ adsorbed volume at $p/p^0 = 0.99$. The specific surface areas and micropore volumes were calculated using the Brunauer–Emmett–Teller (BET) method and t-plot, respectively.

ICP-AES

Chemical compositions of the as-synthesized catalysts were determined by inductively coupled plasma-atomic emission spectroscopy (ICP-AES), using an IRIS 1000 instrument (Thermal Elemental, USA).

NH₃-TPD

The temperature programmed desorption of ammonia (NH₃-TPD) was performed using an AutoChem II 2920 (Micromeritics, USA). Prior to desorption of ammonia, the samples were kept at 373 K in NH₃ flow (30 ml/min) for 40 min. The TPD profiles were determined when heating the samples from 373 to 973 K at a temperature ramp of 15 K/min in He flow (30 ml/min).

Py-IR

Infrared spectra of pyridine adsorption (Py-IR) on Beta zeolites were recorded on a Tensor 27 spectrometer (Bruker, Germany) at 473 K, 573 K and 673 K. The amount of pyridine adsorbed on Brønsted (Py-H⁺) and Lewis (Py-L) acid sites was calculated from integrating the band at 1545 and 1455 cm⁻¹, respectively.^[5]

CO chemisorption

CO chemisorption was measured on an AutoChem 2920 instrument (Micromeritics, USA) at 318 K to determine Pt dispersions of the catalyst samples. The exposed active surface areas of the catalysts were determined via H₂ titration at room temperature. In each experiment, 0.10 g of catalyst was used. The catalyst was reduced in 10% H₂/Ar with a flow rate of 30 mL/min, ramped up at a rate of 10 K/min and then maintained at 723 K for 3 h, before CO chemisorption. After reduction, the catalyst was purged with

SUPPORTING INFORMATION

an ultrahigh-purity helium flow, before being cooled to room temperature. CO pulses were introduced over the reduced catalyst and the CO uptake for each pulse was monitored using a thermal conductivity detector (TCD).

1.3. Catalytic tests

The *n*-heptane isomerization reaction was performed in a fixed-bed reactor at atmospheric pressure and different temperatures, i.e., 515, 529, 538, and 568 K. Prior to the catalytic tests, the reaction conditions were determined to eliminate the diffusion resistances in the catalyst surface film and in the meso- and macropores of the catalyst. The fixed-bed reactor was equipped with a quartz tube with an inner diameter of 6 mm; 0.02 g catalyst powder was well dispersed in 0.18 g silica sand and then this mixture was loaded into the quartz tube. Prior to the reaction, the catalyst was reduced in H₂ flow at 723 K for 2.5 h and subsequently cooled down to the reaction temperature under H₂ flow. Then, *n*-heptane was fed into the reactor by bubbling H₂ in a saturator loaded with liquid *n*-heptane and maintained at 297.5 K, yielding a flow of binary mixture with a *n*-heptane partial pressure of 0.059 atm and weight hourly space velocity (WHSV) of *n*-heptane of 40.8 g_{*n*-heptane} (g_{cat} h)⁻¹. Meanwhile, another flow of H₂ was added to maintain a H₂/*n*-heptane molar ratio of 23.5. The product gas mixture was analyzed by an on-line gas chromatograph (FuLi GC9790, China), equipped with a flame ionization detector (FID) and a HP-PONA capillary column (50 m × 0.2 mm × 0.5 μm).

1.4 ZLC measurements

The apparent diffusivities of *n*-heptane in the two Beta zeolites at 393, 403, 423, and 443 K were measured using the zero length column (ZLC) method developed by Ruthven and co-workers.^[6-8] Firstly, the Beta zeolite, placed between two stainless steel frits, was activated under helium flow at 423 K overnight. After the activation, the sample was initially saturated with *n*-heptane (1.7 vol.%) that was obtained by bubbling helium in a saturator loaded with *n*-heptane and kept at 275 K. Then, the gas flow

SUPPORTING INFORMATION

was switched to pure helium to desorb *n*-heptane, and the transient effluent concentration was measured by a flame ionization detector (FID). The flow rate for desorption was as high as 100 ml/min to minimize the effect of convection. The apparent diffusivity of *n*-heptane (D_{app}) was obtained using a long-time analysis, from the desorption curve, which can be described by:^[6-8]

$$\frac{c}{c_0} = 2L \sum_{n=1}^{\infty} \frac{\exp\left(-\beta_n^2 \frac{D_{app}}{R^2} t\right)}{\left[\beta_n^2 + L(L-1)\right]} \quad (\text{S1}),$$

where c is the transient effluent concentration of *n*-heptane, c_0 is the initial concentration in the effluent, R is the individual crystal radius of the zeolite sample, and t is the desorption time. The eigenvalues β_n in Eq. (S1) are given by:

$$\beta_n \cot(\beta_n) + L - 1 = 0 \quad (\text{S2}),$$

$$L = \frac{1}{3} \frac{FR^2}{KV_s D_{app}} \quad (\text{S3}),$$

where F is the interstitial gas velocity, K is Henry's law constant, and V_s is the solid volume in the ZLC cell. In the long-time regime, Eq. (S1) can be reduced to:

$$\frac{c}{c_0} = \frac{2L}{\beta_1^2 + L(L-1)} \exp\left(-\beta_1^2 \frac{D_{app}}{R^2} t\right) \quad (\text{S4}),$$

where D_{app}/R^2 can be obtained from the long-time slope when plotting $\ln(c/c_0)$ versus time, t .

SUPPORTING INFORMATION

2. Results and Discussion

2.1. Characteristics of Beta samples

Table S2. Characteristics of the two Beta zeolites synthesized in this work.

Properties	Unit	Beta-A	Beta-B
Si/Al ratio ^a	/	24	25
Crystal size obtained from TEM	nm	28	300
Particle size ^b	nm	240	300
S_{BET} ^c	m ² /g	580	680
S_{ext} ^d	m ² /g	120	105
V_{total} ^e	cm ³ /g	0.60	0.43
V_{micro} ^f	cm ³ /g	0.22	0.26
NH ₃ -W ^g	mmol/g	0.023	0.018
NH ₃ -S ^h	mmol/g	0.045	0.040
Py-H ⁺ (473 K) ⁱ	mmol/g	0.161	0.131
Py-L(473 K) ^j	mmol/g	0.214	0.175
Py-H ⁺ (573 K) ^k	mmol/g	0.133	0.098
Py-L(573 K) ^l	mmol/g	0.177	0.131
Py-H ⁺ (673 K) ^m	mmol/g	0.084	0.072
Py-L(673 K) ⁿ	mmol/g	0.112	0.096

^a Si/Al molar ratio measured by using ICP-AES.

^b Average particle size determined from SEM.

^c Specific surface area calculated by BET method.

^d External surface area calculated by t-plot method.

^e Total volume determined from the adsorbed volume at $p/p^0 = 0.99$.

^f Micropore volume calculated by t-plot method.

^{g, h} Weak (NH₃-W) and Strong (NH₃-S) acid sites content calculated from NH₃-TPD.

^{i, j, k, l, m, n} Brønsted (Py-H⁺) and Lewis (Py-L) acid sites content calculated from Py-IR (473, 573 and 673 K).

SUPPORTING INFORMATION

2.2. Pt particle size

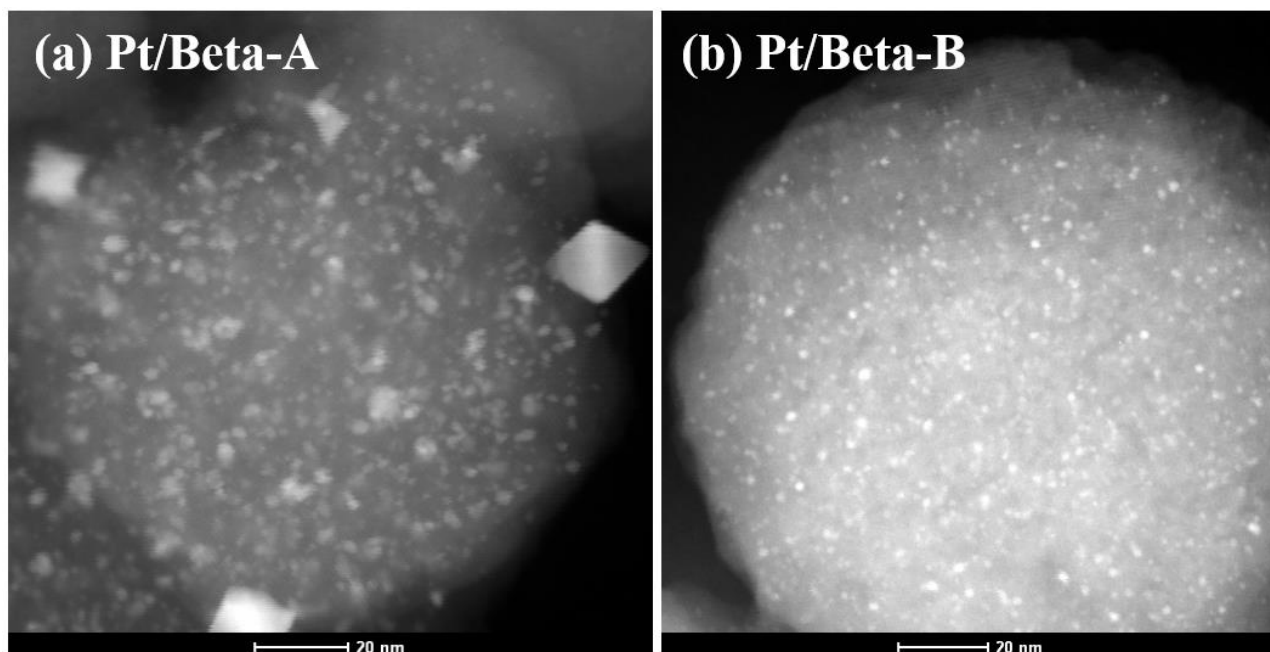


Figure S1. Representative HAADF-STEM images of (a) Pt/Beta-A and (b) Pt/Beta-B.

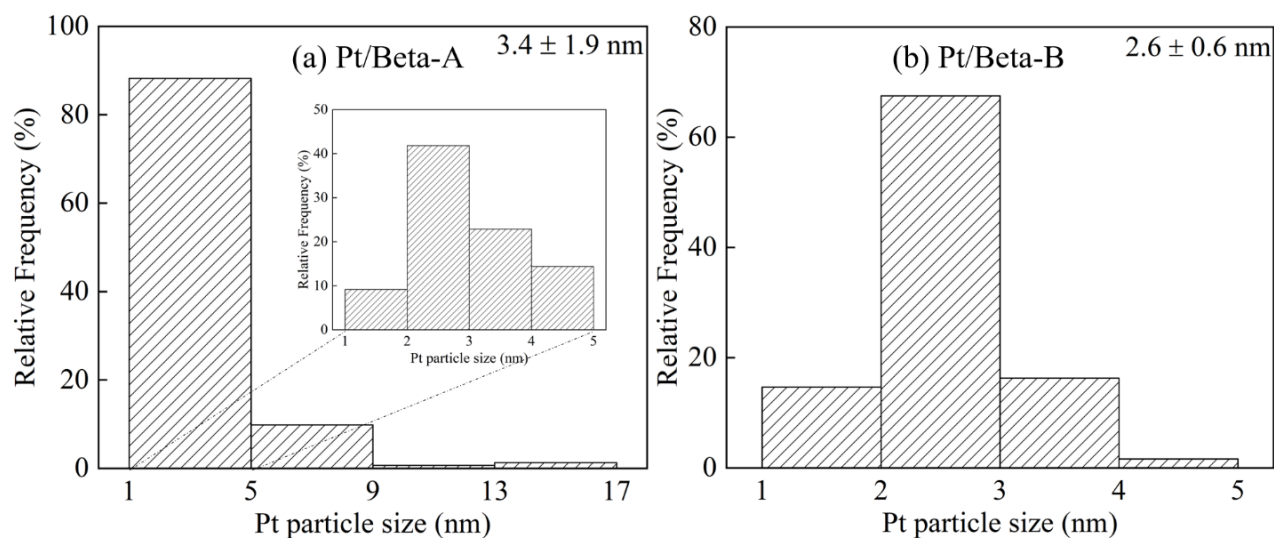


Figure S2. Pt particle size distributions of (a) Pt/Beta-A and (b) Pt/Beta-B. The distributions were determined from HAADF-STEM images.

SUPPORTING INFORMATION

Table S3. Characteristics of Pt particles in Pt/Beta-A and Pt/Beta-B catalysts.

Catalysts	Pt dispersion ^a (%)	Pt particle size ^a (nm)	Pt particle size ^b (nm)
Pt/Beta-A	32	3.5	3.4
Pt/Beta-B	46	2.5	2.6

^a Pt particle size determined by CO chemisorption^b Average Pt particle size determined by HAADF-STEM

SUPPORTING INFORMATION

2.3. Elimination of the effect of Pt

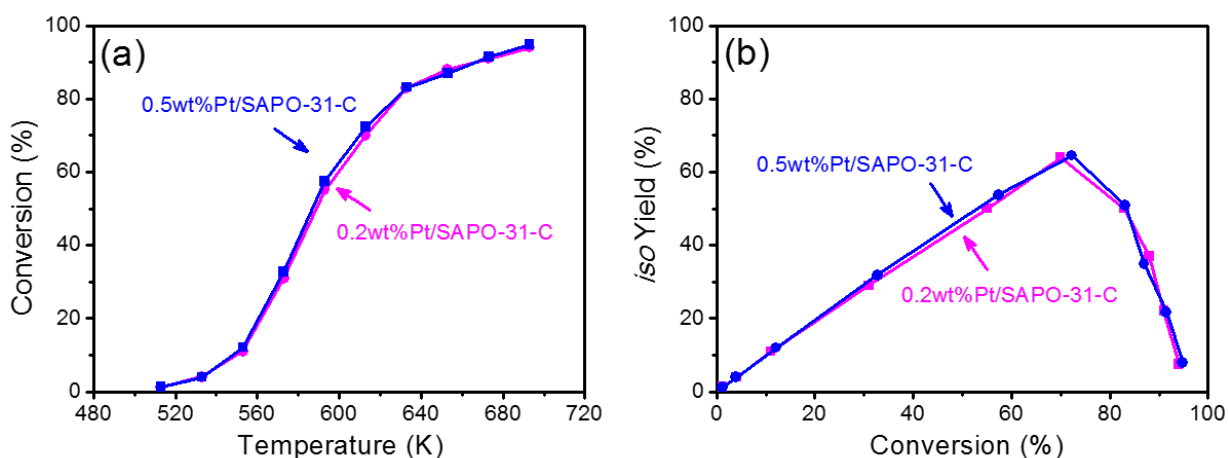


Figure S3. (a) Conversions of *n*-heptane for two Pt/SAPO-31 catalysts with Pt loadings of 0.2 wt% and 0.5 wt% under different reaction temperatures; (b) yields of isomers for two Pt/SAPO-31 catalysts with Pt loadings of 0.2 wt% and 0.5 wt% at different conversions. Reaction conditions: 1.20 g catalyst, $P = 1$ atm, $\text{WHSV} = 1.0 \text{ g}_{n\text{-heptane}} (\text{g}_{\text{cat}} \text{ h})^{-1}$, $\text{H}_2/n\text{-pentane}$ molar ratio = 20. These experimental data are adopted from the work published by our lab^[9].

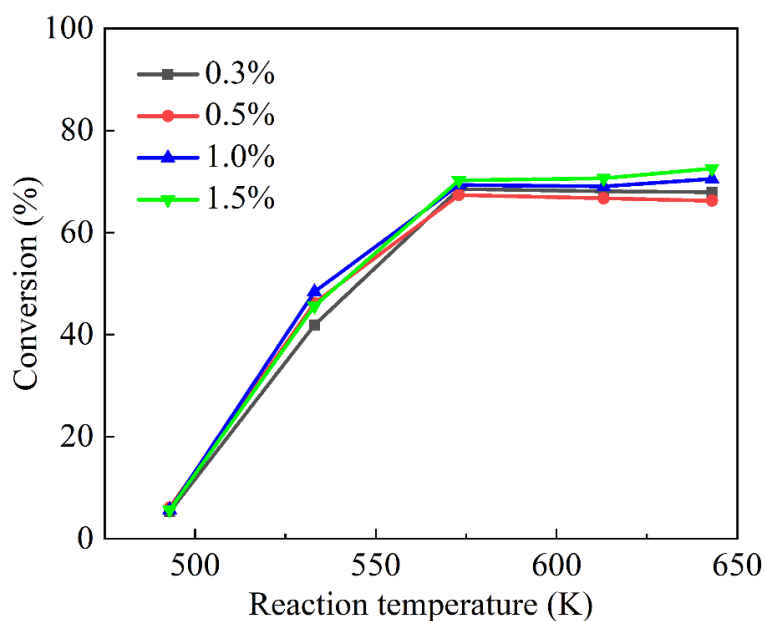


Figure S4. Conversions of *n*-pentane for four Pt/Beta catalysts with different Pt loadings (0.3 wt%, 0.5 wt%, 1.0 wt% and 1.5 wt%) under different reaction temperatures (493 K, 533 K, 573 K, 613 K and 643 K).

SUPPORTING INFORMATION

K). Reaction conditions: 0.3 g catalysts, $P = 1$ atm, $WHSV = 2.3 \text{ g}_{n\text{-pentane}} (\text{g}_{\text{cat}} \text{ h})^{-1}$, $\text{H}_2/n\text{-pentane}$ molar ratio = 2.8. These experimental data are adopted from our previous work^[10].

SUPPORTING INFORMATION

2.4. Catalytic performance

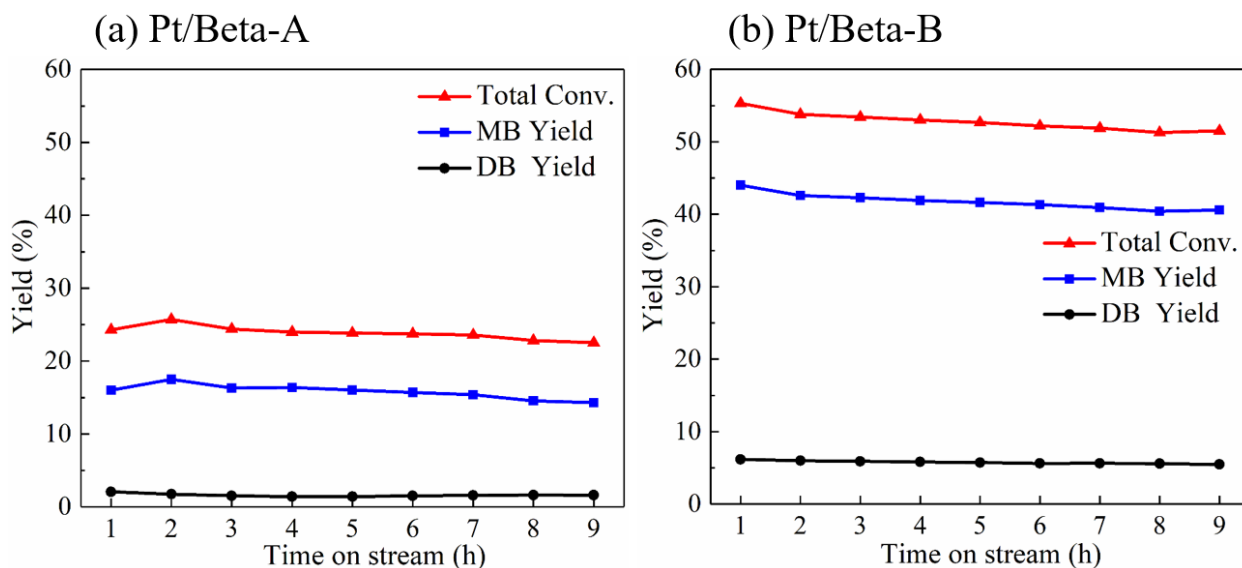


Figure S5. Yields of di-branched isomers (DB) and mono-branched isomers (MB) at different times on stream for (a) Pt/Beta-A and (b) Pt/Beta-B. Reaction conditions: $T = 568$ K, $P = 1$ atm, $\text{WHSV} = 40.8 \text{ g}_{n\text{-heptane}} (\text{g}_{\text{cat}} \text{ h})^{-1}$, $\text{H}_2/n\text{-heptane}$ molar ratio = 23.5.

Table S4. The catalytic performance of Pt/Beta-A and Pt/Beta-B catalysts in catalysing isomerization of n -heptane (Time on stream = 1 h). DB: di-branched isomers; MB: mono-branched isomers.

Catalysts	Temperature (K)	Total conv. (%)	MB Yield. (%)	DB Yield. (%)	Total Sel. (%)
Pt/Beta-A	515	5.6	5.6	—	100
	529	10.2	9.1	0.6	95
	538	11.5	8.9	1.1	87
	568	24.3	16.0	2.1	74
Pt/Beta-B	515	4.9	4.9	—	100
	529	12.5	11.9	0.6	100
	538	15.8	14.3	1.2	98
	568	55.3	44.0	6.2	91

SUPPORTING INFORMATION

2.5. ZLC results

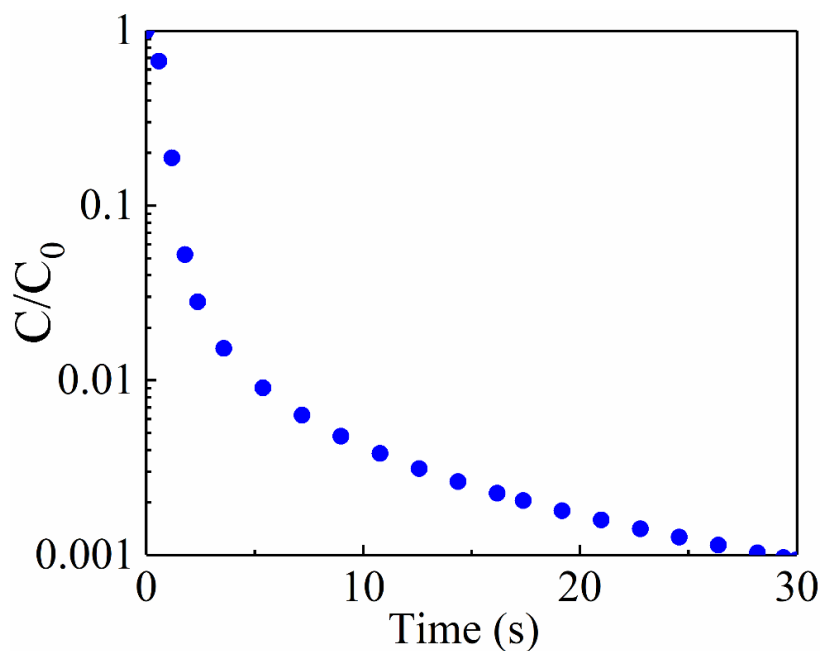


Figure S6. The desorption curve for a blank ZLC experiment conducted at a helium flow rate of 100 ml/min and a temperature of 383 K.

Table S5. Apparent diffusivities and inverses of the diffusion time constants (D_{app}/R^2) of n-heptane in Beta-A and Beta-B at different temperatures.

Temperature (K)	Apparent diffusivity (m ² /s)		Diffusion time constant (s ⁻¹)	
	Beta-A	Beta-B	Beta-A	Beta-B
393	3.43E-18	1.05E-17	2.38E-04	4.67E-04
403	4.66E-18	1.62E-17	3.24E-04	7.20E-04
423	9.86E-18	2.13E-17	6.85E-04	9.47E-04
433	2.16E-17	4.13E-17	1.50E-03	1.84E-03

Table S6. Comparison of the reported D_{app}/R^2 for n-heptane in the literature^[11], and the ones obtained in this work for different samples of Beta zeolites.

Samples	Temperature (K)	Method	D_{app}/R^2 (s ⁻¹)	Ref.
Beta	393	ZLC	5.89E-04	[11]
Beta-A	393	ZLC	2.38E-04	This work
Beta-B	393	ZLC	4.67E-04	This work

SUPPORTING INFORMATION

3. References

- [1] D. Jin, G. Ye, J. Zheng, W. Yang, K. Zhu, M.-O. Coppens, X. Zhou, *ACS Catal.* **2017**, *7*, 5887–5902.
- [2] A. Brito, F. J. García, M. C. Alvarez-Galván, M. E. Borges, C. Díaz, V. A. de la Peña O’Shea, *Catal. Commun.* **2007**, *8*, 2081–2086.
- [3] Z. B. Wang, A. Kamo, T. Yoneda, T. Komatsu, T. Yashima, *Appl. Catal. A Gen.* **1997**, *159*, 119–132.
- [4] C. Woltz, Kinetic Studies on Alkane Hydroisomerization over Bifunctional Catalysts, Technische Universität München, **2005**.
- [5] A. Astafan, M. A. Benghalem, Y. Pouilloux, J. Patarin, N. Bats, C. Bouchy, T. J. Daou, L. Pinard, *J. Catal.* **2016**, *336*, 1–10.
- [6] S. Brandani, D. M. Ruthven, *Adsorption* **1996**, *2*, 133–143.
- [7] J. R. Hufton, D. M. Ruthven, *Ind. Eng. Chem. Res.* **1993**, *32*, 2379–2386.
- [8] M. Eic, D. M. Ruthven, *Zeolites* **1988**, *8*, 40–45.
- [9] T. Yue, W. Liu, L. Li, X. Zhao, K. Zhu, X. Zhou, W. Yang, *J. Catal.* **2018**, *364*, 308–327.
- [10] Y. Sun, Pt/HBeta for n-Pentane Hydroisomerization: Structure-Activity Relationship and Reaction Kinetics, East China University of Science and Technology, **2017**. (Thesis)
- [11] P. M. Lima, C. V Goncalves, C. L. Cavalcante Jr, D. Cardoso, *Microporous Mesoporous Mater.* **2008**, *116*, 352–357.

SUPPORTING INFORMATION

4. Author Contributions

G.Y. and M.-O.C. conceived the initial idea, and G.Y. and Z. G. designed the experiments. Z.G. carried out most of the experiments, including catalyst synthesis, characterization and tests. X.L. and S.H. carried out ZLC measurements and part of the catalyst characterization and tests. X.Z. provided some suggestions to improve the work. G.Y., M.-O.C., Z.G., X.L., and S.H. analyzed the data and wrote the manuscript.